



Cite this: *New J. Chem.*, 2019, 43, 16497

# A benzimidazole-based non-symmetrical tripodal receptor for the ratiometric fluorescence sensing of fluoride ions and solid state recognition of sulfate ions†

Nilotpal Borah, Biswajit Nayak, Abhijit Gogoi and Gopal Das \*

Herein, a novel non-symmetric tripodal receptor has been synthesized and reported as a fluorescent chemosensor for fluoride ions with a remarkable red shift of 100 nm. The receptor was designed with benzimidazole and amide  $\text{-NH}$  functionalities to achieve fluorescence signals during anion sensing; the recognition behaviour of the probe towards fluoride ions was investigated using emission spectroscopy based on a ratiometric change with the limit of detection as low as 0.875 ppb as well as a visual change in colour from violet to cyan under UV light.  $^1\text{H}$  NMR studies confirmed the initial formation of the  $\text{-NH}\cdots\text{F}^-$  hydrogen bond and the subsequent deprotonation of benzimidazole and amide upon the addition of fluoride ions. In addition, an INHIBIT-type logic gate at the molecular level could be fabricated using the reversibility and the reusability of the probe towards the  $\text{F}^-$  and  $\text{H}^+$  ions. Moreover, visual detection of fluoride ions in the solid state was feasible as the receptor-coated TLC plates and paper strips detected the former under UV light. In the protonated form, the asymmetric unit encompasses two molecules of the non-symmetrical receptor that bind two molecules of sulfate anions, and the benzimidazole  $\text{-NH}$ s have been found to be potent hydrogen bond donors.

Received 31st July 2019,  
Accepted 20th September 2019

DOI: 10.1039/c9nj03961a

rsc.li/njc

## Introduction

Selective anion recognition has emerged to be a forefront research topic in the recent past owing to its vital role in chemical, biological, and ecological processes.<sup>1–4</sup> The design of abiotic receptors with enriched anion recognition properties is always a stimulating task primarily because of the different charge to radius ratios, geometries and protonation states of the target anion;<sup>5,6</sup> both neutral and positively charged receptors conventionally comprise organic frameworks containing apposite functionalities with suitable hydrogen bond donors. To recognize and selectively bind the anions in an appropriate framework, most of the neutral artificial receptors establish hydrogen-bonding interactions expending the hydrogen bonds offered by the specific binding sites from amide,<sup>7–9</sup> urea/thiourea,<sup>10,11</sup> pyrrole/indole,<sup>12–15</sup> and imidazole/benzimidazole<sup>16–20</sup> functionalities. Because of its amphoteric nature and sheer presence in the human body as an active site in various histidine- and histamine-containing

metalloproteins, the imidazole core has the capability of binding both anions and cations as well as neutral organic molecules;<sup>21</sup> however, the benzimidazole core is more attractive than the imidazole core because it contains a fluorogenic antenna in addition to protonation sites on the imidazole ring nitrogen, which provides electrostatic assistance during hydrogen bonding interactions. In addition to our constant efforts to synthesize symmetric tripodal receptors comprising urea/thiourea/amide functionalities,<sup>22–24</sup> efforts to synthesize non-symmetric tripodals having different podants have been carried out. The introduction of both benzimidazole and amide  $\text{-NH}$  in a single tripodal receptor for anion binding is a fairly newer idea considering the probability of anion selectivity in both the solid state and the solution phase. In our earlier study, we have demonstrated a non-symmetrical tripodal fabricated with two symmetric arms containing a benzimidazole moiety along with an amide-linked  $\pi$  acidic nitrophenyl moiety.<sup>25</sup> In this study, we modified the third amide-linked arm with a naphthyl residue to improve the photo-physical properties of our previously reported receptor; thus, in addition to providing electronic assistance, the two similar benzimidazole arms provided binding propensity towards anions with their acidic  $\text{-NH}$  protons along with their apparent protonation sites. The third non-symmetric amide-linked arm increased the anion binding aptitude, whereas the naphthyl part improved the fluorogenic responses, which were absent in the earlier case.

Department of Chemistry, Indian Institute of Technology, Guwahati, Assam, 781 039, India. E-mail: gdas@iitg.ac.in

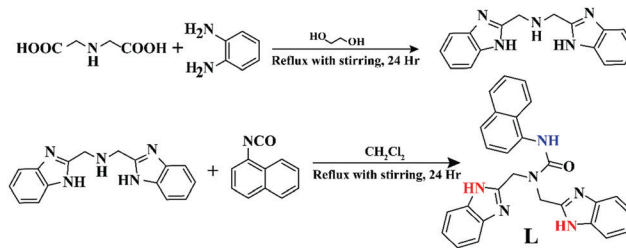
† Electronic supplementary information (ESI) available: Experimental section,  $^1\text{H}$  NMR,  $^{13}\text{C}$  NMR, and mass spectra as characterization data for L, Benesi–Hildebrand plot, Job's plot, LOD calculations, TFA titrations, crystallographic data and refinement details, hydrogen bonding distances. CCDC 1920832 and 1920833. For ESI and crystallographic data in CIF or other electronic format see DOI: 10.1039/c9nj03961a

Among spherical halides, the recognition of fluoride has significant importance as it possesses highest hydration energy among the mono negative species ( $\Delta G_h = -465 \text{ kJ mol}^{-1}$  and  $\Delta H^\circ = 100\text{--}110 \text{ kcal mol}^{-1}$ ).<sup>26</sup> Due to its high solvation enthalpy, the fluoride anion has highest electronegativity, maximum charge density as a chemical entity and a relatively smaller ionic radius (1.47 Å). However, excessive fluoride ions in drinking water may lead to skeletal and dental fluorosis. The presence of fluoride at toxic levels leads to osteosarcoma in the human body,<sup>27</sup> whereas the treatment of osteoporosis can be achieved by fluoride.<sup>28</sup> According to the standards set by the United States Environmental Protection Agency (EPA), drinking water should contain the standard levels of fluoride ions with a maximum level of 4 ppm ( $\sim 200 \mu\text{M}$ ) and a secondary level of 2 ppm ( $\sim 100 \mu\text{M}$ ) to avoid health hazards. Moreover, the Department of Health and Human Services has recommended an optimal fluoride level of 0.7–1.2 ppm for community water systems.<sup>29</sup> In recent years, the design of highly sensitive and selective receptors for the detection and monitoring of fluoride ions has attracted significant interest.<sup>30–35</sup> Colorimetric changes or emission quenching are the major events observed for most of the fluoride sensors;<sup>36–38</sup> however, receptors with emission intensity enhancement are significantly few in number.<sup>39–41</sup> Moreover, one major aspect of fluorescence sensing is to synthesize small molecules capable of the quantitative determination of a specific analyte with evident selectivity. Analysis by a probe with fluorescence measurement at a single wavelength may be impeded by a variety of analyte-independent features such as instrumental parameters, the surrounding microenvironment of the probe, the native concentration of the probe molecule as well as photobleaching. On the contrary, ratiometric fluorescent sensors are more convenient as they enable emission intensity measurement at two different wavelengths; this ensures integrated rectification for environmental effects as well as an upturn in the dynamic range of emission.<sup>42–45</sup> This, in turn, makes the development of ratiometric fluorescent sensors for fluoride anions an interesting research area. Tetrahedral sulfate anions being prominently present in nuclear wastes can interfere in the treatment processes.<sup>46</sup> This anion is also accountable for the permanent hardness of water in addition to ice nucleation phenomenon in the upper atmosphere. Moreover, it plays a substantial role in sulfate binding proteins.<sup>47–49</sup> In this study, our newly synthesized novel non-symmetric tripodal receptor acted as a neutral ratiometric sensor towards the monovalent fluoride anion in the solution phase, whereas in its protonated form, it could selectively bind a sulfate anion in the solid state.

## Results and discussion

### Design principles of the non-symmetrical receptor

Considering the advantages of non-symmetric tripodals, **L** was synthesized (Scheme 1) to enrich the photophysical property of our previously reported receptor, and the solid-state structural variation was also analyzed with various anions of the same.<sup>9</sup> Our former ligand contained a nitrophenyl moiety along with two benzimidazole-containing symmetric arms, whereas the



Scheme 1 Synthetic route to **L**.

newly synthesized receptor **L** possessed an amide-linked naphthyl group as the non-symmetric arm, which was supposed to augment anion binding in the solution phase as well as in the solid state.

### Solution-phase studies of the receptor

**UV-Vis spectra.** The solution of the probe **L** (10  $\mu\text{M}$ ) was taken in a quartz optical cell having an optical path length of 1 cm, and the anion binding properties of the probe were studied by UV/Vis spectroscopy in an acetonitrile solution. The UV-visible spectrum of the probe exhibited two absorption maxima at 276 nm and 282 nm, attributed to  $\pi\text{--}\pi$  transitions in the system. Upon the addition of 10 equivalents of various anions such as  $\text{CH}_3\text{CO}_2^-$  ( $\text{OAc}^-$ ),  $\text{Cl}^-$ ,  $\text{Br}^-$ ,  $\text{I}^-$ ,  $\text{NO}_3^-$ ,  $\text{HCO}_3^-$ ,  $\text{HSO}_4^-$ ,  $\text{SO}_4^{2-}$ ,  $\text{ClO}_4^-$ ,  $\text{PPI}$ ,  $\text{H}_2\text{PO}_4^-$ ,  $\text{PO}_4^{3-}$ , and  $\text{SCN}^-$ , no characteristic change was observed in the original spectrum of the probe. Upon the addition of highly basic TBAF, the absorbance at 282 nm rendered a diminutive change (Fig. S7, ESI<sup>†</sup>). During the addition of this highly basic anion, the corresponding visual colour change occurred *i.e.* the pink-colored ligand solution turned colourless. After having a preview of the colorimetric behaviour of the tripodal probe **L** using different anions, we decided to comprehensively explore the fluorescence sensing ability of this receptor.

**Fluorescence studies.** The tripodal probe exhibited a distinct emission maximum at 373 nm in an acetonitrile solution upon excitation at 285 nm. Similar to the findings of the UV-visible spectral study, *via* the fluorescence study, it was found that the receptor interacted only with the fluoride anion in the excited state, and upon the addition of 10 equivalents of TBAF, a new red-shifted emission maximum was observed at 473 nm with the remarkable Stokes shift of 100 nm (Fig. 1(a)). The resulting solution thus emitted an intense cyan fluorescence, which was easily detectable under a 365 nm UV lamp. However, this selectivity was solvent-dependent, and the sensitivity was negligible in the presence of water or other protic solvents (Fig. S8, ESI<sup>†</sup>). To achieve a quantitative appraisal of the interaction, fluorescence titration experiments were carried out in acetonitrile. The emission intensity at 473 nm increased with a gradual increase in the concentration of fluoride. The intensity at 473 nm kept increasing until it reached a saturation value with the addition of 6 equivalents of fluoride ion. Interestingly, the intensity maximum at 473 nm surpassed the original intensity at 373 nm. As shown in Fig. 1(b), the incremental addition of the TBAF solution created a coinciding scenario, *i.e.* the intensity at 473 nm was switched “on”, whereas the intensity at 373 nm was

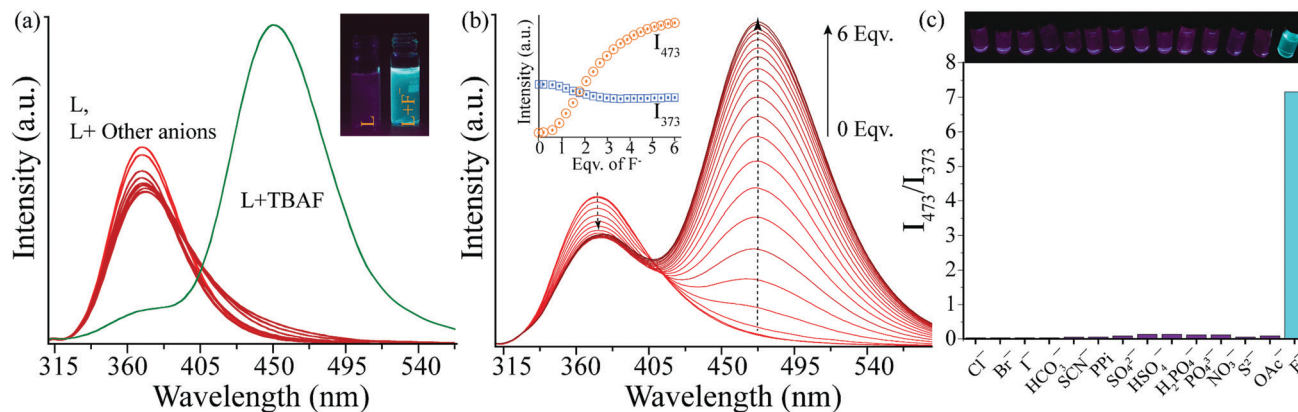


Fig. 1 (a) Changes in the emission spectra of L (10  $\mu$ M) with the incremental addition of TBAF and other anions (10 equivalents) in acetonitrile. Inset: Visible colour change upon the addition of  $F^-$  to L under a UV lamp ( $\lambda_{\text{ex}} = 365$  nm). (b) Fluorescence titration spectra of L upon the incremental addition of 6 equiv. of TBAF in acetonitrile. Inset: Changes in the fluorescence intensity at 373 nm and 473 nm with the incremental addition of TBAF. (c) Colour bars represent the fluorescence intensity ratio  $I_{473}/I_{373}$  upon the addition of 10 equivalents of various anions. The inset shows the corresponding visual fluorescence colour under a UV lamp.

switched “off”, leading to the construction of a ratiometric probe. The ratio between the intensity maximum at 373 nm and that at 473 nm were evaluated and are plotted against their respective anions in Fig. 1(c). However, the fluoride-induced resulting spectra are similar to the hydroxide-added spectra along with their equivalent fluorescence intensity ratio of  $I_{473}/I_{373}$ ; this suggests the deprotonation of this receptor at higher concentrations of fluoride (Fig. S9(a) and (b), ESI $^\dagger$ ). Thus, the ratiometric fluorescence change may occur *via* an enhancement in the extent of intramolecular charge transfer (ICT). The ratiometric probe has several advantages such as high signal-to-noise ratio and ability to detect the analytes irrespective of its concentration. As the probe L involved deprotonation, we also carried out a fluorescence pH titration experiment in an aqueous medium. A ratiometric change similar to that observed upon the addition of TBAF in acetonitrile was apparent at higher pH values of the aqueous medium, whereas in an acidic medium, the intensity of the peak at 373 nm diminished (Fig. S9(c), ESI $^\dagger$ ).

Job's plot derived from the fluorescence titration in acetonitrile suggested the formation of a 1:3 (receptor:fluoride) binding stoichiometry, which corroborated the three apparent binding sites of the receptor (Fig. S10(a), ESI $^\dagger$ ). The binding constant evaluated from the Benesi-Hildebrand equation was found to be  $1.25 \times 10^{17} \text{ M}^{-1}$  for fluoride anions (Fig. S10(b), ESI $^\dagger$ ). The limit of detection (LOD) of the tripodal receptor towards the fluoride anion was evaluated and found to be as low as  $4.63 \times 10^{-8} \text{ M}$  (Fig. S11, ESI $^\dagger$ ) or 0.875 ppb. This LOD value was comparable to or lower than that of the previously reported receptors towards fluoride anions, which are summarised in Table S3, ESI $^\dagger$ .

**$^1\text{H}$  NMR titration studies with the fluoride anion.** Based on the fluorescence studies, it was postulated that the selectivity of the probe towards fluoride was due to the interaction of anions with acidic benzimidazole and amide  $-\text{NHs}$  and subsequent deprotonation of the probe by fluoride at high concentrations. To confirm the aforementioned postulate and study the mechanistic features of the interaction between the probe L and fluoride

ions, the  $^1\text{H}$  NMR titration experiments were conducted in  $\text{DMSO-}d_6$  at a 10 mM concentration of the probe solution with TBAF. Initially, as shown in Fig. 2, upon the addition of fluoride anions at low concentrations (up to 0.8 equiv.), the proton signals of benzimidazole  $-\text{NHs}$ ,  $\text{H}_a$  (13.02 ppm), and amide  $-\text{NH}$ ,  $\text{H}_b$  (9.28 ppm), showed a considerable broadening with significant downfield shifts ( $\Delta\delta = 0.32$  ppm and  $\Delta\delta = 0.35$  ppm), indicating the initial interaction of fluoride ions with the acidic benzimidazole and amide  $-\text{NH}$  protons, respectively. The benzimidazole  $-\text{NH}$  signal vanished first upon the addition of 0.8 equivalent of TBAF, followed by the disappearance of the signal of amide  $-\text{NH}$  upon the addition of 2.0 equivalent of TBAF (Fig. S12, ESI $^\dagger$ ). As the complexation of  $\text{L-H}\cdots\text{F}^-$  occurred, it gradually increased the electron density of the complex. This, in turn, triggered the minute upfield shift of the other aromatic  $-\text{CH}$  proton signals  $\text{H}_d$  and the methylene  $-\text{CH}$  proton signals  $\text{H}_e$  *via* through-bond effects with an increase in the amount of fluoride anions till 2.0 equivalent. After the addition of 2.0 equivalents of TBAF, the deprotonation of the probe L may have started, which is reflected in the more pronounced upfield shift of the two proton signals  $\text{H}_d$  and  $\text{H}_e$ , as depicted in the stacked figure. Moreover, the deprotonation of the probe L upon the addition of excess TBAF can be further supported by the occurrence of a triplet proton signal at 16.02 ppm, confirming the formation of  $\text{HF}_2^-$  species, which is the most stable hydrogen-bonded complex formed by the fluoride ion.<sup>50–52</sup> Interestingly, the doublet of naphthyl  $-\text{CH}$ ,  $\text{H}_c$  at 8.17 ppm, showed a gradual downfield shift, which escalated in the presence of excess TBAF. Again, the changes become more pronounced after the addition of 2.0 equivalents of fluoride anions. This thereby suggests the interaction of the probe L with the fluoride anion after the commencement of its deprotonation. This, in turn, suggests the prominent interaction of the probe with the fluoride anion in the solution phase. Based on the outcomes obtained from the  $^1\text{H}$  NMR study, the sensing mechanism for fluoride ion can be established with the following observations. (i) Initially, at lower fluoride concentrations, benzimidazole and amide  $-\text{NHs}$  form

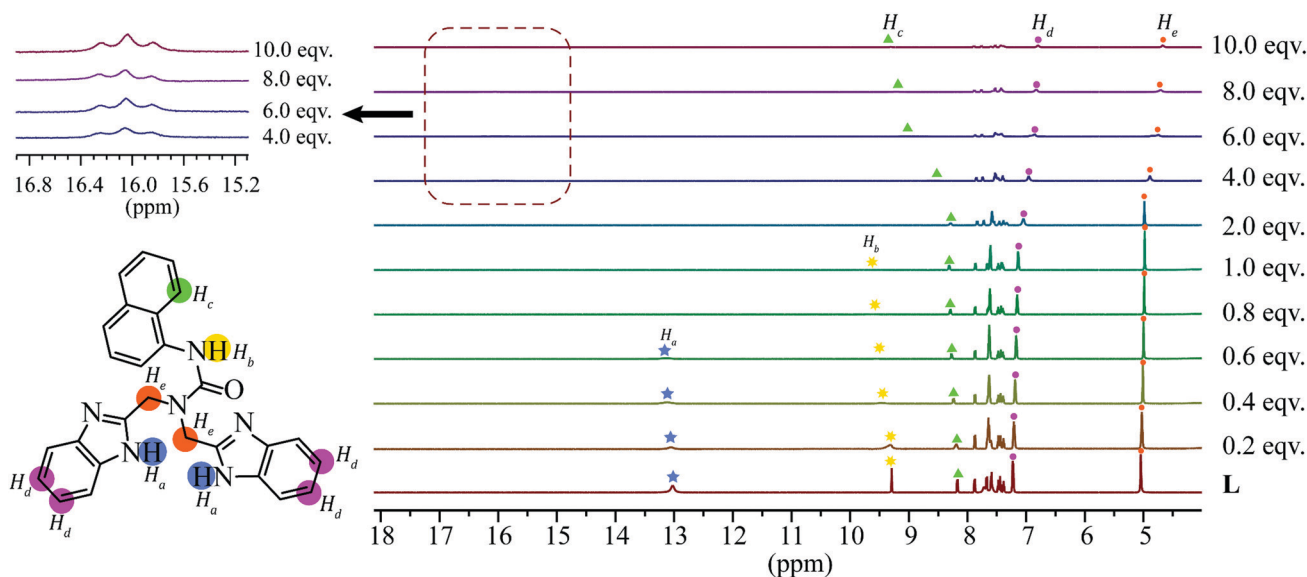


Fig. 2 Stack plot of the  $^1\text{H}$  NMR spectra of the receptor **L** in the presence of increasing amounts of TBAF (1–10 equiv.) obtained in  $\text{DMSO}-d_6$ .

a hydrogen-bonded complex with the fluoride anions, and (ii) then, when excess fluoride is introduced into the receptor-fluoride complex, due to its high affinity towards hydrogen, fluoride can easily bring about the cleavage of the acidic N–H bond, which thereby increases the electron density on both the benzimidazole and the naphthyl moiety.

**Reversible binding and the interpretation of the related logic gate.** To scrutinize the reversibility and reusability of the probe towards the fluoride anion, fluorescence studies of the probe- $\text{F}^-$  with the addition of incremental amounts of TFA (trifluoroacetic acid) were carried out (Fig. S13, ESI $^\dagger$ ). Upon the addition of TFA, an obvious decrease in the intensity at 473 nm along with a simultaneous increase in the original intensity at 373 nm were observed. The fluorescence spectra of the probe- $\text{F}^-$  complex could revert to their free sensor state upon the addition of seven equivalents of TFA. Upon the addition of TFA, the probe finally recovered its original optical properties. Recently, optical switches have attracted significant interest due to their capability in information processing and the manipulation of Boolean-type logic gates at the molecular level.<sup>53,54</sup> The probe **L** exhibited reversibility and recyclability towards the  $\text{F}^-$  and  $\text{H}^+$  ions (Fig. 3(a)); this encouraged us to frame a logic gate based on its distinctive behaviour. Based on the ratiometric fluorescence responses of the probe, a molecular “INHIBIT”-type logic gate was constructed. The addition of  $\text{F}^-$  and  $\text{H}^+$  was considered to be the chemical inputs and denoted as Input 1 (Inp1) and Input 2 (Inp2), respectively. Consequently, as shown in Fig. 3(b),  $I_{473}/I_{373}$ , the ratiometric response between the intensity maximum at 373 nm and that at 473 nm, was taken as the output. The “INHIBIT” (an amalgamated AND and NOT logic gate) logic gate could be fabricated considering a threshold value of 4 for the ratio  $I_{473}/I_{373}$ . As the  $\text{F}^-$  anion induced an “ON” signal in the output, whereas  $\text{H}^+$  regulated the “OFF” signal in the optical output, the ratio  $I_{473}/I_{373}$  with values greater than 4 was considered to be ‘1’ and that with values less than 4 was considered to be ‘0’.

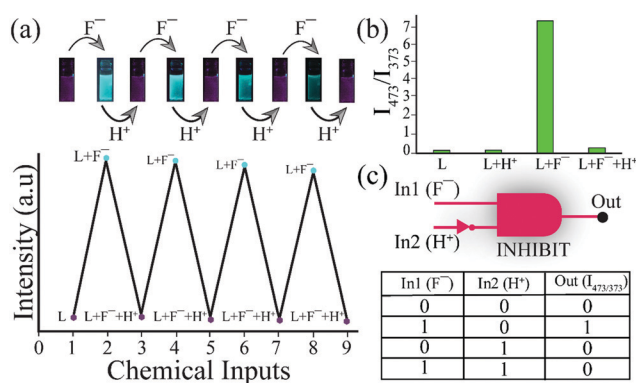


Fig. 3 (a) Reversible and recyclable behaviour of the probe **L** upon the addition of TBAF and TFA. Inset: The corresponding colour changes during alternate cycles. (b) The  $I_{473}/I_{373}$  values for alternate cycles. (c) The fabricated “INHIBIT” logic gate based on the probe behaviour towards  $\text{F}^-$  and  $\text{H}^+$  along with its truth table.

Moreover, when both the  $\text{F}^-$  and  $\text{H}^+$  inputs were missing, ‘0’ was assigned, and in their presence, the inputs were denoted as ‘1’ (Fig. 3(c)).

**Visual detection of the fluoride ion.** In the solid state, visual detection of  $\text{F}^-$  under UV light was also accomplished following the methods reported in the literature.<sup>55,56</sup> As shown in Fig. 4(a), a quantifiable 100 mM solution of the receptor **L** was adsorbed on a thin layer chromatography (TLC) plate, which revealed a violet emission under UV light. Upon the addition of a fluoride ion spot (10 mM), it was adsorbed on the plate, changing the colour to cyan in the center. Thus, the receptor-adsorbed TLC plate served as a prospective sensor to detect the  $\text{F}^-$  ions. To check the feasibility of using sensor-coated Whatman filter paper strips, these strips were dipped into the sensor solution in DMSO (50 mM) and then dried under vacuum.<sup>57,58</sup> The introduction of the coated strips in a 0.1 mM  $\text{F}^-$  solution induced a swift change in its fluorescence colour to cyan under the

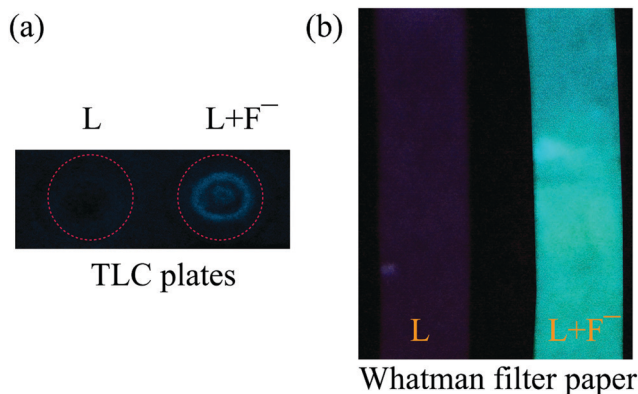


Fig. 4 (a) Fluorescence image (under 365 nm UV light) of the chemosensor adsorbed on a TLC plate and the spot of the TBAF solution on it. (b) Fluorescence changes (under 365 nm UV light) of the test strips in the presence of the TBAF solution.

365 nm UV light (Fig. 4(b)). Thus, it also paves a way towards the development of quick and cheap sensors for fluoride ion in the solid state. These studies strengthen the possible candidature of the probe towards the faster and convenient detection of fluoride ions.

#### Solid-state studies of L and its corresponding salts

**Structure elucidation of the Ligand L.** The non-symmetric tripodal L crystallizes in the  $P\bar{1}$  space group in the triclinic system. Moreover, two units of ligands are present in an asymmetric unit, where each unit adopts a distorted 'T' like structure and is arranged in an alternate 'up-down' fashion mainly due to three types of hydrogen bonds (Fig. 5(a)). In response to the stabilization imposed by the surrounding species, each receptor differs in symmetry equivalence ( $c' = 2$ ); this results in two distinct conformational isomorphs *viz.* C1 (blue coloured) and C2 (green coloured). Generally, conformational isomerism is a result of kinetic and thermodynamic crystal stability factors, which are mostly considered to be the consequences imposed by erratic crystallization, first demonstrated by Desiraju *et al.*<sup>59</sup> The C1 isomorph exhibits intramolecular hydrogen bonding between two benzimidazole arms, whereas it links to another similar unit through hydrogen bonding between benzimidazole nitrogen and amide -NH. In the case of the C2 units, intramolecular -NH...N bonding between the two benzimidazole arms forces these arms to reside in a single plane, whereas the third arm that is adorned with amide -NH protrudes itself out of the plane.

The remaining -NH fragment from the second benzimidazole arm along with one methylene-CH of the same ligand tugs the carbonyl oxygen of the second similar unit of the isomorph and trusses up the two units together (Fig. 5(b)). The interactions between the C1 and the C2 units are composed of hydrogen bonding between the carbonyl oxygen of the amide group and the benzimidazole -NH along with the two fascinating -CH... $\pi$  interactions associated with the benzimidazole and naphthyl -CHs of two different C1 units with the naphthyl ring of the C2 unit. These interactions, in turn, play a crucial role in the development of a three-dimensional structure (Fig. 5(c)). Among these hydrogen bonding interactions, the intramolecular -NH...N bonding interaction between benzimidazole arms in a single unit is strongest.

**Study of the binding of polyatomic anions with  $LH_2^+$ .** All the attempts to study the interactions of the probe- $F^-$  in the solid state with the neutral receptor were unsuccessful due to the deprotonation of the probe. Along with the acidic -NH protons, the receptor L contains apparent protonation sites at the benzimidazole nitrogen atoms. Therefore, attempts were also made with the protonated probe to bind anions in the solid state. Among all the anions, only the protonated salt of  $H_2SO_4$  was obtained.

**Structural study of the complex  $[2(LH_2)^{2+} \cdot 2SO_4^{2-}]$ .** The blue-colored crystal appropriate for the single-crystal XRD analysis was obtained by the reaction of receptor L and  $H_2SO_4$  in DMSO. Structure elucidation by single-crystal XRD discloses that the complex crystallizes in a triclinic system involving the space group  $P\bar{1}$  with  $Z = 4$ . The asymmetric unit comprises two units of protonated receptors and two units of  $SO_4^{2-}$  anions. A total of seven protonated receptors were involved in the formation of a pseudocapsular cavity wherein two pairs of sulfate anions are encapsulated (Fig. 6(b)). The protonated receptors also exhibit conformational isomerism like in the ligand crystal. The two isomorphs link to one another through intermolecular hydrogen bonding interactions between the receptor units and the conjugated anions. The C1 isomorph (blue coloured) attaches itself directly to the C2 isomorph (green coloured) *via* -CH... $\pi$  interaction between the methylene bridge and the naphthyl group. Apart from this, the C1 isomorph offers two hydrogen bonds, whereas C2 donates four hydrogen bonds to the two S2-centered sulfates, which bridge both the conformational isomorphs. Interestingly, in the vicinity of the S1-centered sulfates, all these bonding patterns alter between C1 and C2.

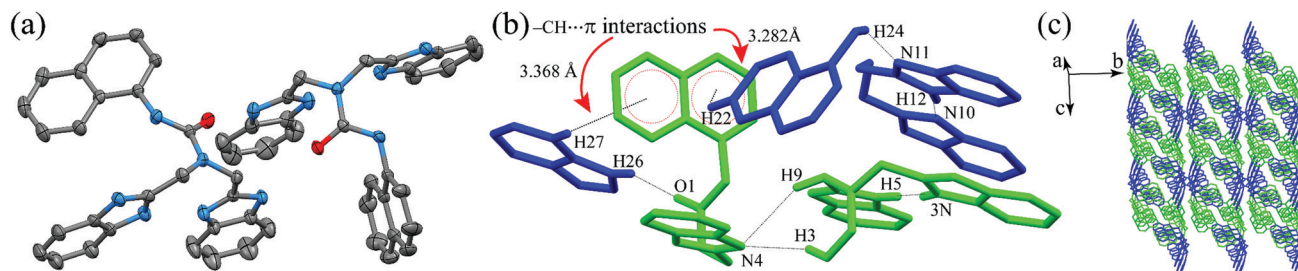


Fig. 5 (a) Ortep diagram of the asymmetric unit of L. (b) Various hydrogen bonding interactions between different isomorphs in the ligand crystal. (c) Packing diagram of the L units along the crystallographic *b* axis.

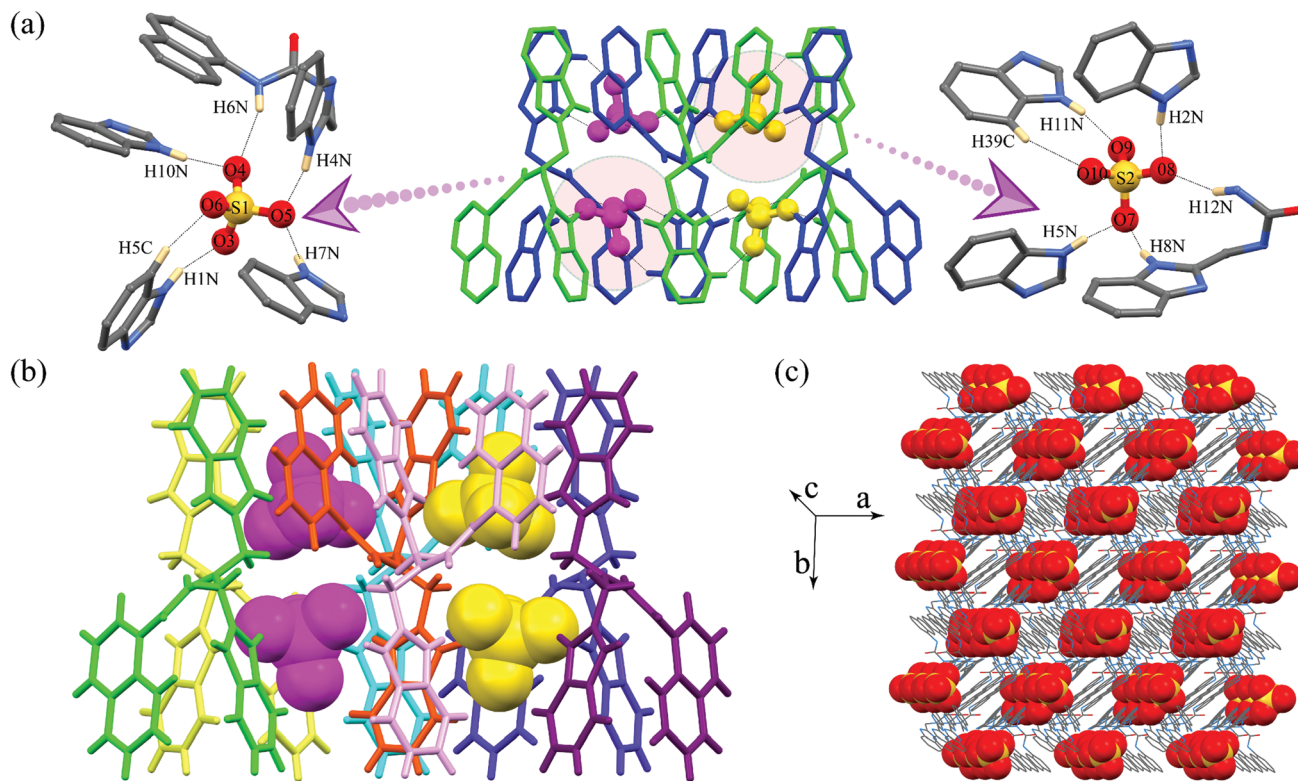


Fig. 6 X-ray structures depicting (a) hydrogen bonding coordination environment of two sulfate anions surrounded by the protonated receptors. (b) Space-fill representation of sulfate anions in the pseudo-encapsulated cavity of protonated receptor. (c) The packing motifs of the sulfate complex as viewed down along the crystallographic *c* axis.

Solitary hydrogen bonding interactions exist between C1 and C2 as the amide  $\text{C}=\text{O}$  of one unit attached itself to the methylene  $\text{CH}$  of the benzimidazole arm. In the cases of both isomorphs, one connects to another similar unit using one  $\text{CH}\cdots\pi$  interaction between the naphthyl and the benzimidazole moiety (Fig. S14, ESI<sup>†</sup>), whereas the hydrogen bond between amide  $\text{C}=\text{O}$  and naphthyl  $\text{CH}$  plays a pivotal role in decorating the three-dimensional structure (Fig. 6(c)). As evident from Fig. 6(c), the two sulfates experience different binding environments, surrounded by three units of C1 isomorphs and four units of C2 isomorphs. Considering the binding environment of the S1-centered sulfate in the crystal structure, it is apparent that it is coordinated by six valid hydrogen bonds. The significant interactions are from five benzimidazole and amide-linked  $\text{NH}\cdots\text{O}$  (average  $\text{N}\cdots\text{O} = 2.750 \text{ \AA}$ ) and one  $\text{CH}\cdots\text{O}$  interactions ( $\text{C}\cdots\text{O} = 3.264 \text{ \AA}$ ). O3 of the bound sulfate is coordinated to one benzimidazole arm *via* a single  $\text{NH}\cdots\text{O}$  interaction. The O4 binding interactions are composed of one unit of benzimidazole-NH and one unit of amide-NH. The bifurcated O5 is hydrogen bonded to two benzimidazole-NHs, whereas the monofurcated O6 is hydrogen bonded to one aromatic  $\text{CH}$  of the benzimidazole group. Among these hydrogen bonding interactions, the stronger hydrogen bonds are donated by the benzimidazole-NH interactions ( $\text{N10H}\cdots\text{O4} = 1.82 \text{ \AA}$ ,  $\angle \text{N-H}\cdots\text{O} = 171.0^\circ$ ;  $\text{N7H}\cdots\text{O5} = 1.83 \text{ \AA}$ ,  $\angle \text{N-H}\cdots\text{O} = 163.0^\circ$ ;  $\text{N4H}\cdots\text{O5} = 1.83 \text{ \AA}$ ,  $\angle \text{N-H}\cdots\text{O} = 163.0^\circ$ ;  $\text{N1H}\cdots\text{O3} = 1.87 \text{ \AA}$ ,  $\angle \text{N-H}\cdots\text{O} = 163.0^\circ$ ), shadowing the amide-NH interaction ( $\text{N6H}\cdots\text{O4} = 2.22 \text{ \AA}$ ,  $\angle \text{N-H}\cdots\text{O} = 158.0^\circ$ ). The surrounding

environment of S2 also depicts a total of six valid binding interactions primarily from five  $\text{NH}\cdots\text{O}$  (average  $\text{N}\cdots\text{O} = 2.748 \text{ \AA}$ ) and one  $\text{CH}\cdots\text{O}$  ( $\text{C}\cdots\text{O} = 3.274 \text{ \AA}$ ). O7 of the bound sulfate is bifurcated with two benzimidazole-NHs. The bifurcated nature of O8 is contributed by the hydrogen bonds donated by one benzimidazole-NH and one amide-NH. O9 is connected to the protonated receptor solely through one benzimidazole-NH. O10 atom of the bound S2 is offered one single hydrogen bond from the one  $\text{CH}$  from benzimidazole group of the protonated receptor. Similar to the case of the S1 environment, benzimidazole-NHs prevail the stronger hydrogen bond donor towards bound S2 centered oxygen atoms. Moreover, four benzimidazole-NHs interactions *viz.*  $\text{N5H}\cdots\text{O7} = 1.85 \text{ \AA}$ ,  $\angle \text{N-H}\cdots\text{O} = 163.0^\circ$ ;  $\text{N8H}\cdots\text{O7} = 1.81 \text{ \AA}$ ,  $\angle \text{N-H}\cdots\text{O} = 165.0^\circ$ ;  $\text{N2H}\cdots\text{O8} = 1.82 \text{ \AA}$ ,  $\angle \text{N-H}\cdots\text{O} = 168.0^\circ$ ;  $\text{N11H}\cdots\text{O9} = 1.86 \text{ \AA}$ ,  $\angle \text{N-H}\cdots\text{O} = 164.0^\circ$  show greater hydrogen bonding aptitude towards the encapsulated anion than the potential amide-NH interaction ( $\text{N12H}\cdots\text{O8} = 2.24 \text{ \AA}$ ,  $\angle \text{N-H}\cdots\text{O} = 157.0^\circ$ ). All the oxygen atoms of the S1 and S2-centered sulfates are consistent with the electronic structure calculations reported by Hay *et al.*, suggesting the involvement of a maximum of three hydrogen bonds for each oxygen atom of an oxo anion.<sup>60</sup>

## Conclusion

In brief, we efficaciously designed and synthesized a novel non-symmetric tripodal receptor that acted as a selective fluoride

ion sensor in the solution phase. The recognition behaviour of the probe in acetonitrile towards fluoride ion was investigated using emission spectroscopy and based on visual change in colour from violet to cyan under UV lamp. Selectivity towards the fluoride anion was achieved through the selective formation of a hydrogen-bonded host-guest complex with the consequent deprotonation of the probe. The  $^1\text{H}$  NMR experiments with the  $\text{F}^-$  ion indicated that the deprotonation of the probe was facilitated by the inherent acidity of benzimidazole and amide  $-\text{NH}$ , the basic nature of the fluoride ion and the polarity of the acetonitrile solvent. The reversibility and reusability of the probe towards  $\text{F}^-$  and  $\text{H}^+$  led to the fabrication of an INHIBIT-type molecular logic gate. Fluoride ion detection in the solid state was also accomplished *via* a TLC plate and solution-coated paper strips. Since the deprotonation of the probe played a pivotal role in the solution phase detection of fluoride ions, the protonation of the probe led to the detection of sulphate anions in the solid state. In the solid-state study, the asymmetric unit incorporates one pair of non-symmetrical protonated receptors, which exist as conformational isomorphs tending to bind two units of sulfate anions. Moreover, two different binding environments were present in the case of the two bound sulfates, where the strongest hydrogen bonds are offered by the benzimidazole  $-\text{NH}$  moiety.

## Conflicts of interest

There are no conflicts to declare.

## Acknowledgements

The financial support provided by DBT, New Delhi, India, through grant BT/COE/34/SP28408/2018 is highly acknowledged. Authors would like to acknowledge the Central Instruments Facility of IIT Guwahati and DST FIST for X-ray crystallography. NB, BN and AG acknowledge IIT Guwahati for fellowship.

## Notes and references

- P. A. Gale, Anion receptor chemistry: highlights from 2008 and 2009, *Chem. Soc. Rev.*, 2010, **39**, 3746–3771.
- M. Wenzel, J. R. Hiscock and P. A. Gale, Anion receptor chemistry: highlights from 2010, *Chem. Soc. Rev.*, 2012, **41**, 480–520.
- P. A. Gale, E. N. W. Howe and X. Wu, Anion Receptor Chemistry, *Chem.*, 2016, **1**, 351–422.
- P. A. Gale, E. N. W. Howe, X. Wu and M. J. Spooner, Anion receptor chemistry: Highlights from 2016, *Coord. Chem. Rev.*, 2018, **375**, 333–372.
- K. Bowman-James, A. Bianchi and E. Garcia-España, *Anion Coordination Chemistry*, Wiley-VCH, New York, ch. 1–2, 2011.
- P. D. Beer and P. A. Gale, Anion Recognition and Sensing: The State of the Art and Future Perspectives, *Angew. Chem., Int. Ed.*, 2001, **40**, 486–516.
- S. O. Kang, R. A. Begum and K. Bowman-James, Amide-based ligands for anion coordination, *Angew. Chem., Int. Ed.*, 2006, **45**, 7882–7894.
- S. O. Kang, M. A. Hossain and K. Bowman-James, Influence of dimensionality and charge on anion binding in amide-based macrocyclic receptors, *Coord. Chem. Rev.*, 2006, **250**, 3038–3052.
- K. Choi and A. D. Hamilton, Selective Anion Binding by a Macrocyclic with Convergent Hydrogen Bonding Functionality, *J. Am. Chem. Soc.*, 2001, **123**, 2456–2457.
- J. W. Steed, Anion-tuned supramolecular gels: a natural evolution from urea supramolecular chemistry, *Chem. Soc. Rev.*, 2010, **39**, 3686–3699.
- A. F. Li, J. H. Wang, F. Wang and Y. B. Jiang, Anion complexation and sensing using modified urea and thiourea-based receptors, *Chem. Soc. Rev.*, 2010, **39**, 3729–3745.
- I. Saha, J. T. Lee and C.-H. Lee, Recent Advancements in Calix[4]pyrrole-Based Anion-Receptor Chemistry, *Eur. J. Org. Chem.*, 2015, 3859–3885.
- H. Maeda, T. Shirai, Y. Bando, K. Takaishi, M. Uchiyama, A. Muranaka, T. Kawai and M. Naito, Chiroptical Control in Helical Receptor–Anion Complexes, *Org. Lett.*, 2013, **15**, 6006–6009.
- P. A. Gale, J. R. Hiscock, C. Z. Jie, M. B. Hursthouse and M. E. Light, Acyclic indole and carbazole-based sulfate receptors, *Chem. Sci.*, 2010, **1**, 215–220.
- R. Manivannan, A. Satheshkumar, E. H. El-Mossalamy, L. M. Al-Harbi, S. A. Kosa and K. P. Elango, Design, synthesis and characterization of indole based anion sensing receptors, *New J. Chem.*, 2015, **39**, 3936–3947.
- Z. Xu, S. K. Kim and J. Yoon, Revisit to imidazolium receptors for the recognition of anions: highlighted research during 2006–2009, *Chem. Soc. Rev.*, 2010, **39**, 1457–1466.
- N. Kumari, S. Jha and S. Bhattacharya, Colorimetric Probes Based on Anthraimidazolediones for Selective Sensing of Fluoride and Cyanide Ion via Intramolecular Charge Transfer, *J. Org. Chem.*, 2011, **76**, 8215–8222.
- P. A. Gale, J. R. Hiscock, N. Lalaoui, M. E. Light, N. J. Wells and M. Wenzel, Benzimidazole-based anion receptors: tautomeric switching and selectivity, *Org. Biomol. Chem.*, 2012, **10**, 5909–5915.
- N. Singh and D. O. Jang, Benzimidazole-Based Tripodal Receptor: Highly Selective Fluorescent Chemosensor for Iodide in Aqueous Solution, *Org. Lett.*, 2007, **9**, 1991–1994.
- Z. Guo, R. Song, J. H. Moon, M. Kim, E. J. Jun, J. Choi, J. Y. Lee, C. W. Bielawski, J. L. Sessler and J. Yoon, A Benzobisimidazolium-Based Fluorescent and Colorimetric Chemosensor for  $\text{CO}_2$ , *J. Am. Chem. Soc.*, 2012, **134**, 17846–17849.
- I. Bertini, A. Sigel and H. Sigel, *Handbook on Metalloproteins*, Marcel and Dekker, New York, 2001.
- S. K. Dey and G. Das, A selective fluoride encapsulated neutral tripodal receptor capsule: solvatochromism and solvatomorphism, *Chem. Commun.*, 2011, **47**, 4983–4985.
- A. Basu and G. Das, A  $C_{3v}$ -Symmetric Tripodal Urea Receptor for Anions and Ion Pairs: Formation of Dimeric Capsular Assemblies of the Receptor during Anion and Ion Pair Coordination, *J. Org. Chem.*, 2014, **79**, 2647–2656.
- S. K. Dey, R. Chutia and G. Das, Oxyanion-Encapsulated Caged Supramolecular Frameworks of a Tris(urea) Receptor:

- Evidence of Hydroxide- and Fluoride-Ion-Induced Fixation of Atmospheric CO<sub>2</sub> as a Trapped CO<sub>3</sub><sup>2-</sup> Anion, *Inorg. Chem.*, 2012, **51**, 1727–1738.
- 25 N. Borah, A. Gogoi and G. Das, Competitive anion binding aptitude of benzimidazole and amide functionality of a non-symmetrical receptor in solid state and solution phase, *Supramol. Chem.*, 2016, **28**, 275–283.
- 26 Y. Marcus, Thermodynamics of solvation of ions. Part 5.—Gibbs free energy of hydration at 298.15 K, *J. Chem. Soc., Faraday Trans.*, 1991, **87**, 2995.
- 27 S. Ayooob and A. K. Gupta, Fluoride in Drinking Water: A Review on the Status and Stress Effects, *Crit. Rev. Environ. Sci. Technol.*, 2006, **36**, 433.
- 28 K. L. Kirk, *Biochemistry of the Elemental Halogens and Inorganic Halides*, Plenum Press, New York, 1991, pp. 221–238.
- 29 K. Sebelius, Proposed HHS Recommendation for Fluoride Concentration in Drinking Water for Prevention of Dental Caries, *Fed. Regist.*, 2011, **76**, 2383–2388.
- 30 P. Das, A. K. Mandal, M. K. Kesharwani, E. Suresh, B. Ganguly and A. Das, Receptor design and extraction of inorganic fluoride ion from aqueous medium, *Chem. Commun.*, 2011, **47**, 7398–7400.
- 31 H. Li, R. A. Lalancette and F. Jäkle, Turn-on fluorescence response upon anion binding to dimesitylboryl-functionalized quaterthiophene, *Chem. Commun.*, 2011, **47**, 9378–9380.
- 32 S. Rochat and K. Severin, A simple fluorescence assay for the detection of fluoride in water at neutral pH, *Chem. Commun.*, 2011, **47**, 4391–4393.
- 33 R. Hu, J. Feng, D. H. Hu, S. Q. Wang, S. Y. Li, Y. Li and G. Q. Yang, A Rapid Aqueous Fluoride Ion Sensor with Dual Output Modes, *Angew. Chem., Int. Ed.*, 2010, **49**, 4915–4918.
- 34 M. Cametti and K. Rissanen, Highlights on contemporary recognition and sensing of fluoride anion in solution and in the solid state, *Chem. Soc. Rev.*, 2013, **42**, 2016–2038.
- 35 Y. Zhou, J. F. Zhang and J. Yoon, Fluorescence and Colorimetric Chemosensors for Fluoride-Ion Detection, *Chem. Rev.*, 2014, **114**, 5511–5571.
- 36 E. J. Cho, B. J. Ryu, Y. J. Lee and K. C. Nam, Visible Colorimetric Fluoride Ion Sensors, *Org. Lett.*, 2005, **7**(13), 2607–2609.
- 37 S. Madhu and M. Ravikanth, Boron-Dipyrrromethene Based Reversible and Reusable Selective Chemosensor for Fluoride Detection, *Inorg. Chem.*, 2014, **53**, 1646.
- 38 S. K. Sarkar, S. Mukherjee and P. Thilagar, Going beyond Red with a Tri- and Tetracoordinate Boron Conjugate: Intriguing Near-IR Optical Properties and Applications in Anion Sensing, *Inorg. Chem.*, 2014, **53**, 2343.
- 39 B. Sui, B. Kim, Y. Zhang, A. Frazer and K. D. Belfield, Highly Selective Fluorescence Turn-On Sensor for Fluoride Detection, *ACS Appl. Mater. Interfaces*, 2013, **5**, 2920–2923.
- 40 M. Hirai, M. Myahkostupov, F. N. Castellano and F. P. Gabbaï, 1-Pyrenyl- and 3-Perylenyl-antimony(v) Derivatives for the Fluorescence Turn-On Sensing of Fluoride Ions in Water at Sub-ppm Concentrations, *Organometallics*, 2016, **35**, 1854–1860.
- 41 Y. Jo, N. Chidalla and D.-G. Cho, Bis-ureidoquinoline as a Selective Fluoride Anion Sensor through Hydrogen-Bond Interactions, *J. Org. Chem.*, 2014, **79**, 9418–9422.
- 42 B. C. Zhu, F. Yuan, R. X. Li, Y. M. Li, Q. Wei, Z. M. Ma, B. Du and X. L. Zhang, A highly selective colorimetric and ratiometric fluorescent chemodosimeter for imaging fluoride ions in living cells, *Chem. Commun.*, 2011, **47**, 7098–7100.
- 43 Y. Kubo, M. Yamamoto, M. Ikeda, M. Takeuchi, S. Shinkai, S. Yamaguchi and K. Tamao, A colorimetric and ratiometric fluorescent chemosensor with three emission changes: fluoride ion sensing by a triarylborane–porphyrin conjugate, *Angew. Chem., Int. Ed.*, 2003, **42**, 2036–2040.
- 44 A. K. Mahapatra, P. Karmakar, J. Roy, S. Manna, K. Maiti, P. Sahoo and D. Mandal, Colorimetric and ratiometric fluorescent chemosensor for fluoride ions based on phenanthroimidazole (PI): spectroscopic, NMR and density functional studies, *RSC Adv.*, 2015, **5**, 37935–37942.
- 45 S. Biswas, M. Gangopadhyay, S. Barman, J. Sarkar and N. D. P. Singh, Simple and efficient coumarin-based colorimetric and fluorescent chemosensor for F-detection: An ON1–OFF–ON2 fluorescent assay, *Sens. Actuators, B*, 2016, **222**, 823–832.
- 46 E. A. Katayev, Y. A. Ustynyuk and J. L. Sessler, Receptors for tetrahedral oxyanions, *Coord. Chem. Rev.*, 2006, **250**, 3004.
- 47 H. Weingartner, E. U. Franck, G. Wiegand, N. Dahmen, G. Schwedt, F. H. Frimmel, B. C. Gordalla, K. Johannsen, R. S. Summers, W. Holl, M. Jekel, R. Gimbel, R. Rautenbach and W. H. Glaze, *Ullman's Encyclopedia of Industrial Chemistry*, Wiley-VCH Verlag GmbH & Co., 2000.
- 48 B. A. Moyer and R. P. Singh, *Fundamentals and Applications of Anion Separations*, Kluwer Academic, New York, 2004, pp. 107–114.
- 49 B. A. Moyer, R. Custelcean, B. P. Hay, J. L. Sessler, K. Bowman-James, V. W. Day and S.-O. Kang, A Case for Molecular Recognition in Nuclear Separations: Sulfate Separation from Nuclear Wastes, *Inorg. Chem.*, 2013, **52**, 3473–3490.
- 50 A. B. Descalzo, K. Rurack, H. Weisshoff, R. Martínez-Mañez, M. D. Marcos, P. Amorós, K. Hoffmann and J. Soto, Rational Design of a Chromo- and Fluorogenic Hybrid Chemosensor Material for the Detection of Long-Chain Carboxylates, *J. Am. Chem. Soc.*, 2005, **127**, 184–200.
- 51 X. Zheng, W. Zhu, D. Liu, H. Ai, Y. Huang and Z. Lu, Highly selective colorimetric/fluorometric dual-channel fluoride ion probe, and its capability of differentiating cancer cells, *ACS Appl. Mater. Interfaces*, 2014, **6**, 7996–8000.
- 52 C. Saravanan, S. Easwaramoorthi, C.-Y. Hsiow, K. Wang, M. Hayashi and L. Wang, Benzo-selenadiazole fluorescent probes-near-IR optical and ratiometric fluorescence sensor for fluoride ion, *Org. Lett.*, 2014, **16**, 354–357.
- 53 A. P. De Silva, H. Q. N. Gunaratne and C. P. McCoy, A molecular photoionic AND gate based on fluorescent signalling, *Nature*, 1993, **364**, 42–44.
- 54 B. Kumar, M. A. Kaloo, A. R. Sekhar and J. Sankar, A selective fluoride sensor and a digital processor with “Write–Read–Erase–Read” behaviour, *Dalton Trans.*, 2014, **43**, 16164–16168.

- 55 Y.-C. Wu, J.-P. Huo, L. Cao, S. Ding, L.-Y. Wang, D.-R. Cao and Z.-Y. Wang, Design and application of tri-benzimidazolyl star-shape molecules as fluorescent chemosensors for the fast-response detection of fluoride ion, *Sens. Actuators, B*, 2016, **237**, 865–875.
- 56 Y.-C. Wu, J.-Y. You, K. Jiang, J.-C. Xie, S.-L. Li, D. Cao and Z.-Y. Wang, Colorimetric and ratiometric fluorescent sensor for F<sup>-</sup>-based on benzimidazole-naphthalene conjugate: Reversible and reusable study & design of logic gate function, *Dyes Pigm.*, 2017, **140**, 47–55.
- 57 J.-F. Xiong, J.-X. Li, G.-Z. Mo, J.-P. Huo, J.-Y. Liu, X.-Y. Chen and Z.-Y. Wang, Benzimidazole derivatives: selective fluorescent chemosensors for the picogram detection of picric acid, *J. Org. Chem.*, 2014, **79**, 11619–11630.
- 58 B. Sui, B. Kim, Y. Zhang, A. Frazer and K. D. Belfield, Highly selective fluorescence turn-on sensor for fluoride detection, *ACS Appl. Mater. Interfaces*, 2013, **5**, 2920–2923.
- 59 G. R. Desiraju, Crystal Engineering: A Holistic View, *Angew. Chem., Int. Ed.*, 2007, **47**, 8342–8356.
- 60 B. P. Hay, T. K. Firman and B. A. Moyer, Structural Design Criteria for Anion Hosts: Strategies for Achieving Anion Shape Recognition through the Complementary Placement of Urea Donor Groups, *J. Am. Chem. Soc.*, 2005, **127**, 1810–1819.